# HIGH ENERGY GAMMA RAY BALLOON INSTRUMENT

D.J. Thompson, R.G. Baker, D.L. Bertsch, J.R. Chesney,
S.M. Derdeyn, C.H. Ehrmann, C.E. Fichtel, S.D. Hunter,
J.S. Jacques, N.A. Laubenthal, R.W. Ross
Code 662, NASA/Goddard Space Flight Center
Greenbelt, Maryland 20771 U.S.A

1. Introduction. The High Energy Gamma Ray Balloon Instrument was built in part to verify certain subsystems' performance for the Energetic Gamma Ray Experiment Telescope (EGRET) instrument, the high energy telescope to be carried on the Gamma Ray Observatory (1). This paper describes the instrument, the performance of some subsystems, and some relevant results.

2. Instrument Description. The instrument is similar in size to EGRET and has the basic elements of a conventional high energy $\gamma$-ray telescope. However, being a test vehicle and constrained by the weight and cost limitations of a balloon program, it is much more austere than EGRET. It has, for example, only 12 spark chamber modules (Figure 1), compared to the 36 on EGRET. A $\gamma$-ray entering from above produces no signal in the anticoincidence scintillator "A", but may convert to an electron-positron pair in one of the plates interleaved with the upper 10 spark chamber modules. The electron and positron trigger the coincidence system consisting of scintillators "B", "C", and "D" with the proper time of flight signature between "B" and "C". The inclusion of the "D" signal was optional and commandable. The coincidence signal is used to initiate the high voltage pulse to the spark chambers and the readout of the $\gamma$-ray event. The basic information about the $\gamma$-ray, arrival direction and estimated energy, is derived from the reconstructed picture of the electron and positron trajectories in the spark chamber. Each of the eight pair production plates is a sheet of 0.08 radiation length lead, supported on a grid of stretched high-strength steel wires. The spark chambers have an active area of 81 cm by 81 cm, are of the wire grid design with magnetic core readout and are essentially identical to those being used on the EGRET instrument.

The anticoincidence counter consists of three pieces of scintillator which form a five sided box around the upper spark chamber assembly. The placement of the anti-coincidence system inside the pressure vessel reduces weight and is far less costly than the machined and polished dome surrounding the entire upper portion of the EGRET instrument. The shorter, modular design of the balloon anticoincidence is not as effective as the monolithic dome and it therefore

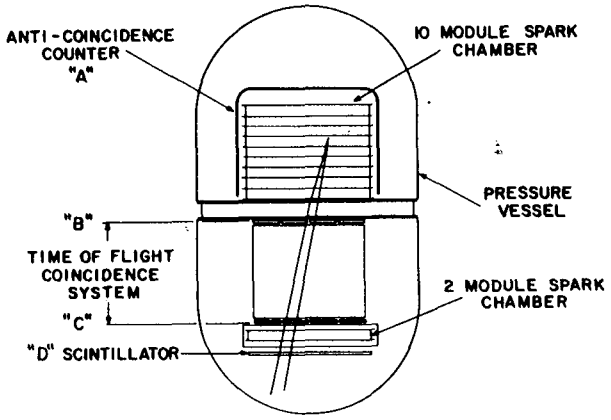


Figure 1 -- Schematic diagram of the High Energy Gamma Ray Balloon Instrument

represents a more severe test of its ability to screen out unwanted events.

The "B" and "C" parts of the triggering system each consist of an array of 16 scintillator tiles in a 4 by 4 pattern. Each tile has its own light pipe and phototube. This coincidence system serves two purposes: (1) The allowed combinations of "B" and "C" tiles define the instrument aperture. (2) These scintillator planes are operated in a time-of-flight arrangement which requires that the particles pass through the "B" plane before the "C" plane, i.e., they must be downward moving. The performance of this coincidence system is discussed in Section 3. The EGRET coincidence system uses the same 4 by 4 scintillator arrays and an almost identical time-of-flight electronics system. The "D" detector is a single unit of plastic scintillator which may be used to verify that at least one of the particles penetrates the entire detector.

The active detectors are contained in a pressure vessel made of aluminum honeycomb with Kevlar face sheets. This composite vessel is lightweight and low density (area density less than 0.5 g $cm^{-2}$) yet capable of being evacuated to remove contaminants. The upper portion of the vessel and the lower spark chamber area are filled with a spark chamber gas mixture (98.5% neon, 0.75% ethane, 0.75% argon), while the region containing the coincidence scintillator, phototubes, and electronics is filled with air. The active area is approximately 6560 $cm^2$ with an area efficiency factor of about 1800 $cm^2$ (E> 400 MeV) The instrument size is 3 m by 1.6 m diameter. With its gondola, it weighs 1300 kg. Balloon flights which provide the results reported here were launched from Palestine, Texas.

## 3. Relevant Subsystems.

a. Spark Chamber. The individual modules have 992 wires in each plane, giving a positional resolution of about 0.4 mm for spark location. The modules are made entirely of low-outgassing materials with the beams themselves being made of Macor. An extensive effort was made in developing techniques for stacking, holding, and determining the alignment of the spark chambers, so that the absolute pointing direction of the assembly could be determined with high precision. The use of a set of optical refererences allowed the absolute pointing direction to be determined to an arcmin. The techniques which have been used in the EGRET development are a direct successor. The performance of the spark chambers is seen in Fig. 2, which shows the electron-positron pair resulting from a high energy $\gamma$ ray interaction. The vertical scale has been compressed in the figure by a factor of 4.7.

b. Time-of-flight coincidence system. The time-of-flight measurement is an important discriminator against unwanted triggers. Each of the 32 tile signals from the "B" and "C" arrays is sent to a constant fraction discriminator. The discriminator signals are summed for each array (with propagation times matched). The time difference between the total "B" signal and the total "C" signal is then digitized using a circuit similar to previous experiments (2). With a 75 cm separation, the time difference between upward-moving and downward-moving particles is 5

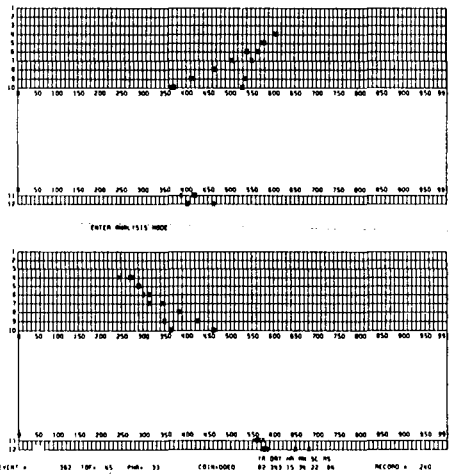

Figure 2 - Orthogonal views of a γ-ray pair production event in the spark chamber.

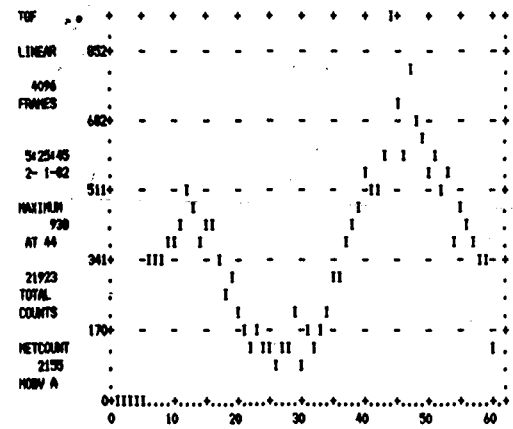


Figure 3 - Time of flight histogram for neutral events during one balloon flight.

nsec. The acceptance threshold for the time difference is adjustable by command. The discrimination, summation, digitization, and comparison is completed in about 400 nsec and is included in the trigger signal to the spark chamber. A histogram of the time-of-flight measurements is accumulated in the data system and regularly telemetered to the ground station. A sample histogram for neutral events, taken directly from the Ground Support Equipment display, is shown in Figure 3. The peak to the right represents downward-moving γ rays and is well separated from the upward-moving peak to the left.

c. Anticoincidence System. As noted in Section 2, the anticoincidence scintillator on the High Energy Gamma Ray Balloon Instrument does not surround the upper layer of the time-of-flight coincidence system, in contrast to other instruments such as SAS-2, COS-B, and EGRET. This short anticoincidence system was recognized as a negative design aspect, because horizontal or even partially downward moving particles could interact above the upper layer of the coincidence system and produce a downward moving particle within the instrument aperture.

An approximate model of predicted event rates was developed from the data of SAS-2 and tested on previous balloon instruments. When applied to the geometry and material factors of this instrument, this model gave the predicted rates which are shown in Table 1, which also shows the observed event rates during a balloon flight. The model did not take into account the different characteristics of this anticoincidence system from all the others.

The overall agreement between the predicted and observed event rate is an indication that the short anticoincidence system was not a major limitation of the instrument. The differences in the types of events seen is probably in large part the result of the anticoincidence configuration, for which no correction was made in the model. The fraction of events which are recognizable γ rays is also high compared

Table I

| Type of Event | Predicted Events/s | Observed Events/s |
|---|---|---|
| Gamma Ray pairs (1) | 1.1 | 0.9 |
| Upper Wall Events (2) | 0.9 | 0.6 |
| Scattered single tracks (3) | 0.8 | 0.8 |
| Other (4) | 0.6 | 1.0 |

(1) Recognizable pairs. The prediction includes atmospheric $\gamma$ rays and $\gamma$ rays produced in the outer instrument shell.
(2) Tracks originating in the walls of the upper chamber.
(3) This number is generally consistent with the expected number of low energy Compton $\gamma$-rays plus pair production $\gamma$-rays for which one track is too short to meet the acceptance criteria.
(4) This category includes short single tracks, multiple single tracks, and events with little information.

to earlier balloon instruments. This favorable rate of useful events was predicted by the model based on the better active volume to wall ratio and to the improved directional recognition of the time-of-flight system. The similarity of this balloon instrument to the EGRET instrument and the known superior aspects of EGRET strongly suggest that EGRET will also have a high fraction of useful events.

d. Automatic Data Processing. The majority of the data for a high energy $\gamma$-ray telescope are the spark chamber pictures. A set of programs, originally developed for the SAS-2 instrument and since refined, analyze the event pictures by pattern recognition. These programs efficiently screen out pictures which do not contain useful information and identify the track structure of potential $\gamma$-ray events, such as the one shown in Fig. 2. Even though the information content of this instrument is low compared to other $\gamma$-ray telescopes, the results of the automatic analysis showed that this program works very well even here, both in selecting desired events and structuring them correctly.

4. Summary. The High Energy Gamma Ray Balloon Instrument has provided a flight test of an austere version of the EGRET telescope. The results have proven the instrument subsystems and approaches and have assisted in the development of assembly procedures used for EGRET.

5. Acknowledgements. We thank George Simpson and Bill Cruickshank for their valuable assistance in the early stages of the program. Our thanks go also to the National Scientific Balloon Facility, Palestine, Texas, for their flight support.

6. References

1. Fichtel, C.E., et al. 1983, ICRC, Paper T1-10, p. 19.
2. Ross, R.W., and Chesney, J.R., 1979, IEEE Trans. Nuc. Sci, NS-27, p.370.